LA-UR- 11-05025

Approved for public release; distribution is unlimited.

Title: Left-right loading dependence of shock response of (111)//(112) Cu bicrystals: deformation and spallation

Author(s): W. Z. Han, Q. An, S. N. Luo, T. C. Germann, D. L. Tonks, W. A. Goddard III

Intended for: Journal of Applied Physics

Los Alamos
NATIONAL LABORATORY
EST. 1943

Los Alamos National Laboratory, an affirmative action/equal opportunity employer, is operated by the Los Alamos National Security, LLC for the National Nuclear Security Administration of the U.S. Department of Energy under contract DE-AC52-06NA25396. By acceptance of this article, the publisher recognizes that the U.S. Government retains a nonexclusive, royalty-free license to publish or reproduce the published form of this contribution, or to allow others to do so, for U.S. Government purposes. Los Alamos National Laboratory requests that the publisher identify this article as work performed under the auspices of the U.S. Department of Energy. Los Alamos National Laboratory strongly supports academic freedom and a researcher's right to publish; as an institution, however, the Laboratory does not endorse the viewpoint of a publication or guarantee its technical correctness.

Form 836 (7/06)

Submitted to *Journal of Applied Physics*

Left-right loading dependence of shock response of (111)//(112) Cu bicrystals: deformation and spallation

W. Z. Han,[1] Q. An,[2] S. N. Luo,[1,*] T. C. Germann,[1] D. L. Tonks,[1] and W. A. Goddard III[2]

[1]*Los Alamos National Laboratory, Los Alamos, NM 87545, USA*

[2]*Materials and Process Simulation Center, California Institute of Technology, Pasadena, CA 91125, USA*

(Dated: August 24, 2011)

Abstract

We investigate with molecular dynamics the dynamic response of Cu bicrystals with a special asymmetric grain boundary (GB), (111)//(112)⟨110⟩, and its dependence on the loading directions. Shock loading is along the GB normal either from the left or right of the GB. Due to the structure asymmetry, the bicrystals demonstrate overall strong left-right loading dependence of its shock response, including compression wave features, compression and tensile plasticity, damage characteristics including spall strength, effective wave speeds and structure changes, except that spallation remains dominated by the GB damage regardless of loading direction.

It is almost axiomatic that microstructure (defects and interfaces) plays a critical role in materials deformation and damage. Given their relative simplicity, bicrystals serve as model systems for studying grain boundary (GB) effect on shock-induced deformation and spallation (simply termed as shock response). Molecular dynamics (MD) simulations are advantageous in revealing real-time atomistic scale phenomena and mechanisms not accessible by current experimental techniques;[1] for example, we utilized MD recently to investigate shock response of Pd bicrystals with a symmetric $\Sigma 5$ GB.[2] In shock loading (as opposed to quasistatic loading), the directionality of wave propagation likely gives rises to the loading-direction dependence of shock response in the presence of structural asymmetry as manifested by an asymmetric GB. We thus investigate with MD a special asymmetric GB, $(111)//(112)\langle 110\rangle$ [Fig. 1(a)]. This involves different GB normals ($\langle 111\rangle$ and $\langle 112\rangle$) and thus different crystallographic directions for wave propagation across this GB, and also $\{111\}$ slip planes oriented differently in the constituent single crystals, raising the possibility that plastic deformation and damage might show left-right loading dependence (LRLD). Indeed, our results show pronounced LRLD overall, a combined effect of the microstructure and wave propagation.

Our MD simulations use an accurate embedded-atom-method potential for Cu[3] with the LAMMPS (large-scale atomic/molecular massively parallel simulator) package.[4] The $(111)//(112)[\bar{1}10]$ GBs were synthesized recently,[5] and are peculiar in that the coincidence-site-lattice method for constructing GBs is not applicable. We thus create separately two grains, Grain I with (111) GB plane and Grain II with $(11\bar{2})$ GB plane, and then combine them to form a bicrystal. The x-, y- and z- axes are along [111], $[11\bar{2}]$ and $[\bar{1}10]$ in Grain I and along $[11\bar{2}]$, [111] and $[\bar{1}10]$ in Grain II, respectively [Fig. 1(a)]. We start with two single crystal supercells, $96\times12\times20$ Grain I (552 960 atoms or $\sim$600 Å$\times$100 Å$\times$100 Å in edge lengths) and $68\times17\times20$ Grain II (554 880 atoms or $\sim$600 Å$\times$100 Å$\times$100 Å in edge lengths), which match in their y-edge lengths. To find the lowest energy GB configuration, we fix Grain I and translate Grain II along three directions in small steps under three-dimensional boundary conditions, within one atom layer spacing in each direction. For each scan, we perform single-point energy calculation and find that the local energy minimum is located at Δx=0.7 Å, Δy=5.9 Å and Δz=0.6 Å (shifting Grain II with respect to its as-constructed position).

For spallation simulations, two single crystal flyer plates identical to Grains I and II

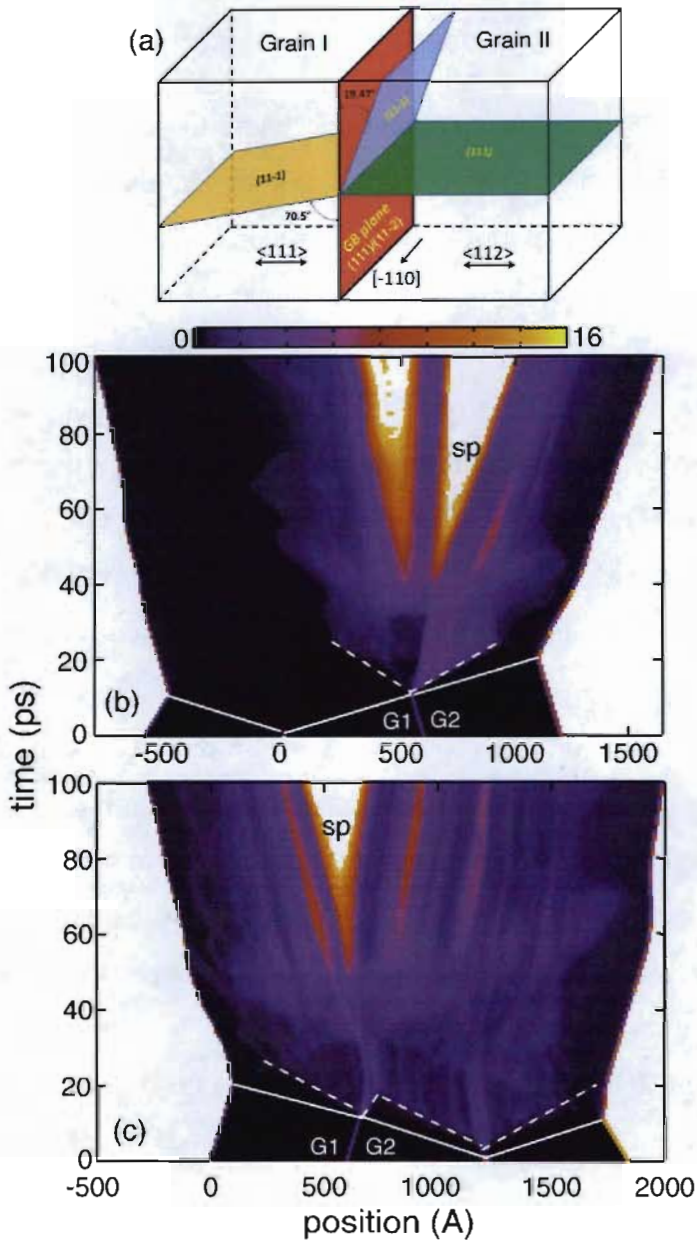

FIG. 1. (a) Schematic configuration of the Cu bicrystal. Shock is along the GB normal from its left (G1 loading) or right (G2 loading). (b)-(c) The x-t diagrams in terms of CSP for u_p=0.75 km/s; (b) is for G1 loading and (c) for G2 loading. Impact plane is at x=0 (b) or x=1200 Å (c). The white solid lines indicate the elastic waves, and the dashed lines, plastic waves. sp: spall region.

are also created for impact on Grain I (referred to as the left or G1 loading) and Grain II (the right or G2 loading) of the bicrystal, respectively. We perform constant-pressure-temperature simulations on the bicrystal and flyer plates at 150 K and 1 atm for 500 ps before shock simulations. A flyer plate and the bicrystal are assembled along the x-axis

(about 1.7 million atoms, or 1800 Å×100 Å×100 Å in edge lengths), and the GB is located at $x \approx 600$ Å (the middle of the bicrystal). We then assign initial velocities of $\pm\frac{2}{3}u_{\rm p}$ and $\mp\frac{4}{3}u_{\rm p}$ along the x-axis to the bicrystal (target) and flyer plate for impact simulations, respectively. Here $u_{\rm p}$ denotes the desired "piston velocity." Shock simulations are performed with the microcanonical ensemble, and periodic boundary conditions are only applied along the y- and z-axes. The time step for integrating the equation of motion in all simulations is 1 fs. The local structure is characterized with the centrosymmetry parameter (CSP)[6] and coordination number. We use the one-dimensional binning analysis to obtain the wave profiles such as stress (σ_{ij}) profiles. Free surface velocity ($u_{\rm fs}$) histories are extracted from the movement of the target free surface (on Grain I or II). The von Mises stress $\sigma_{\rm vM}$ is defined as $(\sigma_{11} - \frac{1}{2}\sigma_{22} - \frac{1}{2}\sigma_{33})$. The spall strength $\sigma_{\rm sp}$ for a given loading is the maximum tensile stress $|\sigma_{11}|$ where spallation occurs. Similar simulation and analysis details can be found elsewhere.[7]

Shock simulations are conducted at $u_{\rm p}$=0.375, 0.5 and 0.75 km/s for each loading geometry. This impact yields shock waves propagating into the bicrystal and the flyer plate, which are then reflected at the respective free surfaces as centered rarefaction fans. These two release fans interact in the bicrystal (near the GB), inducing an evolving tensile region and spallation in the target for sufficiently strong shocks; spallation leads to recompression (even shocks) and free surface velocity pullback. These wave propagation and interactions are illustrated in Figs. 1(b), 1(c) and 2 in terms of the position-time (x-t) diagrams, $u_{\rm fs}(t)$ and stress profiles, showing such feature as shock compression, plastic deformation, release fans, and spallation. Waves may undergo reflection and scattering while crossing GB which may be manifested in different components of, e.g., stress tensor and particle velocity. Our main interest is how the GB asymmetry and the presence or absence of directionality of loading (compression and tension) affect LRLD of dynamic response of the bicrystal.

For shock compression, the shocks are directional, so LRLD is expected and indeed well manifested in particular for high $u_{\rm p}$. The first wave arriving at the GB is elastic. It induces negligible GB plasticity for $u_{\rm p}$=0.375 km/s, so $u_{\rm fs}(t)$ is similar both for G1 and G2 loading while minor differences do exist [Figs. 2(a) and 2(b)]. At higher $u_{\rm p}$, the elastic shock induces two waves (elastic and plastic) after passing the GB, and the GB plasticity increases with increasing $u_{\rm p}$. For G1 loading at 0.5 km/s, the amplitudes of the elastic and plastic waves in Grain II are so close that effectively one wave is observed in $u_{\rm fs}(t)$, and the two-wave structure

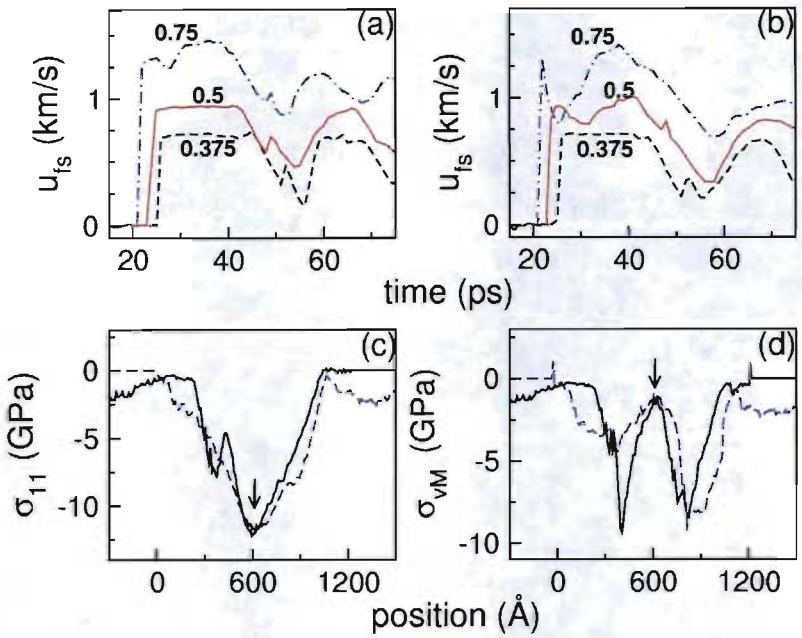

FIG. 2. $u_{\rm fs}(t)$ (a)-(b), and $\sigma_{11}(x)$ during tension (c)-(d). (a)-(b): (a) is for G1 loading and (b) for G2 loading; numbers denote $u_{\rm p}$ in km/s. (c)-(d): $\sigma_{11}(x)$ (c) and $\sigma_{\rm vM}(x)$ (d) for $u_{\rm p}$=0.5 km/s at t=39 ps and 41 ps, respectively; the solid line denotes G1 loading and the dashed line, G2 loading.

becomes pronounced at 0.75 km/s [Fig. 2(a)]. For G2 loading at 0.5 km/s and 0.75 km/s, the elastic-plastic wave feature is more pronounced, but the elastic-plastic transition initiated from the GB is more sluggish (in Grain I) than that for G1 loading (in Grain II) [Figs. 2(a) and 2(b)]. One reason is likely that the slip system is more difficult to activate in Grain I for G2 loading, given the geometry of {111} slip planes [Fig. 1(a)]. The preexisting dislocation partials [Fig. 3(a)] in Grain II near the GB also facilitate the elastic-plastic transition in Grain II for G1 loading. As a result, the plastic wave plateau is narrow for G2 loading [Fig. 2(b)]. For single crystals, Grain I has higher yield strength than Grain II, so two waves (elastic and plastic) are induced in Grain II before they impinge on the GB at $u_{\rm p}$=0.75 km/s for G2 loading, while only a single elastic wave is observed in Grain I for G1 loading [Figs. 1(b) and 1(c)]. Interestingly, the plastic shock initiated from the Grain II interior appears to be impeded by the GB, which is thus both a source and a barrier to dislocations [Fig. 1(c)]. The above observations point to strong LRLD in shock compression response of the (111)//(112)⟨110⟩ bicrystals, in particular when the GB plasticity is involved.

The release fans approach the GB from both sides and induce release and tension. Therefore, the tensile loading lacks directionality. At high $u_{\rm p}$ (e.g., 0.75 km/s), the microstructure

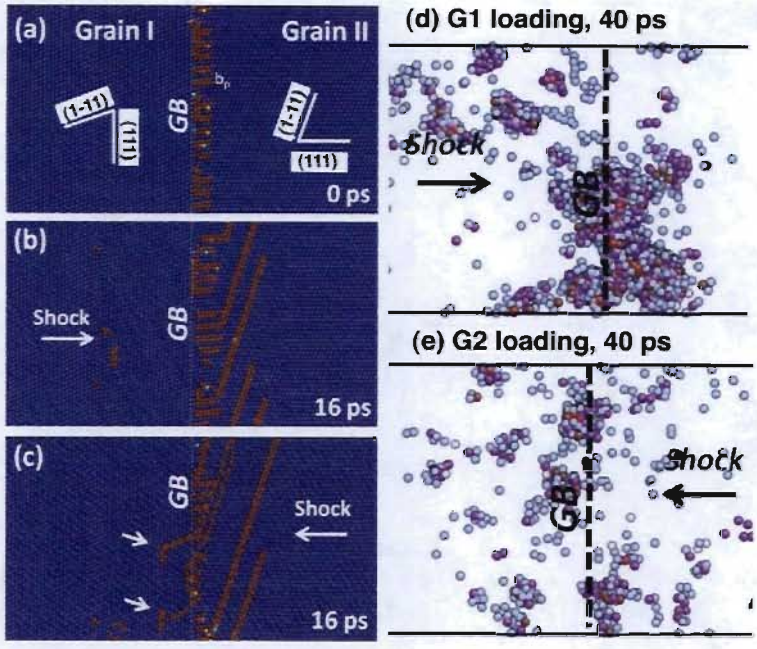

FIG. 3. Snapshots of the bicrystal configuration during shock compression (a)-(c), and spallation (d)-(e) for u_p=0.5 km/s and different loading directions. (a)-(c) use CSP for visualization. Only surface atoms enclosing nanovoids (coordination number below 8) are shown in (d) and (e). Visualization adopts AtomEye.[8]

near the GB undergoes modifications during compression, release and tension before spallation, via compressional and tensile plasticity. For low u_p(e.g., 0.375 km/s), compression plasticity is negligible or modest and tensile plasticity is localized around GB with minor modification to the GB region. Regardless of u_p, the GB is the weakest and located in the maximum tension region, so spallation occurs first at GB with the maximum damage [Figs. 1(b), 1(c) and 2(c)]. The spall "plane" corresponds to the region with maximum shear stress relaxation [comparing Figs. 2(c) and 2(d)] and maximum plasticity. σ_{sp} is about 11.6, 12.1 and 13 GPa for G1 loading (corresponding to u_p=0.375, 0.5 and 0.75 km/s, respectively), slightly higher than those for G2 loading (10, 11.5 and 11.9 GPa, respectively), due to the more pronounced GB plasticity for G2 loading. The spallation occurs later in G2 loading than G1 loading and this delay increases with increasing u_p [Figs. 1(b), 1(c), 2, 3(d) and 3(e)], likely because the overall plasticity is more pronounced in G2 loading and the effective wave speeds are reduced [Figs. 1(b) and 1(c)]. Spallation may occur off the GB, and the off-GB spallation also shows LRLD [Figs. 1(b) and 1(c)].

The atomic configurations in Fig. 3 illustrate further the structure features during compression and tension, using u_p=0.5 km/s as an example. In this bicrystal, there are preexistent partial dislocations in Grain II commonly observed for the $\langle 112 \rangle$ GB plane [Fig. 3(a)]. For shock compression, the GB plasticity triggered by the elastic shock dominates on Grain II side for both loading directions, while the GB plasticity in Grain I is more pronounced for G2 loading than G1 loading [Figs. 3(b) and 3(c); the slanted arrows]. Thus, the more "predamage" (prior to spall) in the GB region for G2 loading leads to smaller σ_{sp}. Figs. 3(d) and 3(e) compare void nucleation/growth at the same time for two loading directions. Spallation in G1 loading leads that in G2 loading for the reason discussed above. While the main voids nucleate on the GB, more secondary voids nucleate in Grain I than Grain II, since more slip systems are activated in Grain I and their interactions initiate vacancies and disordering for void nucleation.[1,9,10] In contrast, the special orientation of Grain II gives rise to preferred shear localization along the $(1\bar{1}1)$ planes [Figs. 3(b) and 3(c)], and thus less slip systems are activated. During tension, we also observe for G1 loading that microtwins form and propagate toward Grain II free surface and induce a transient surface step, but not for G2 loading. This again points to LRLD due to the structural asymmetry.

In summary, our MD simulations of a special asymmetric GB, $(111)//(112)\langle 110 \rangle$, demonstrate strong LRLD of its shock response overall, including compression wave features, compression and tensile plasticity, damage characteristics including spall strength, effective wave speeds, and structure changes. However, spallation is still dominated by the GB damage and this feature lacks LRLD as expected.

This work was supported by the ASC and LDRD programs at LANL, and the PSAAP program at Caltech.

---

* sluo@lanl.gov

[1] S. G. Srinivasan, M. I. Baskes, and G. J. Wagner, J. Appl. Phys. **101**, 043504 (2007).

[2] H. H. Pam, B. Arman, S. N. Luo, and T. Cagin, J. Appl. Phys. **109**, 086107 (2011).

[3] Y. Mishin, M. J. Mehl, D. A. Papaconstantopoulos, A. F. Voter, and J. D. Kress, Phys. Rev. B **63**, 224106 (2001).

[4] http://lammps.sandia.gov.

[5] Y. C. Wang, Z. X. Sun, and D. H. Ping, J. Mater. Sci. Technol. **26**, 1047 (2010).

[6] C. L. Kelchner, S. J. Plimpton, and J. C. Hamilton, Phys. Rev. B **58**, 11085 (1998).

[7] S. N. Luo, Q. An, T. C. Germann, and L. B. Han, J. Appl. Phys. **106**, 013502 (2009).

[8] J. Li, Modell. Simul. Mater. Sci. Eng. **11**, 173 (2003).

[9] S. N. Luo, T. C. Germann, and D. L. Tonks, J. Appl. Phys. **106**, 123518 (2009).

[10] Y. Ashkenazy and R. S. Averback, Appl. Phys. Lett. **86**, 051907 (2005).